Conformations of Bombolitins I and III in Aqueous Solutions: Circular Dichroism, ^{1}H NMR, and Computer Simulation Studies†

Eleni Bairaktari,‡ Dale F. Mierke,§ Stefano Mammi, and Evaristo Peggion*

Biopolymer Research Center, Department of Organic Chemistry, University of Padova, Via Marzolo 1, 35131 Padova, Italy

Received January 17, 1990; Revised Manuscript Received June 28, 1990

ABSTRACT: The heptadecapeptides bombolitin I and bombolitin III are two of a series of peptides postulated to be biologically active within a membrane environment. In the preceding paper [Bairaktari, E., Mierke, D. F., Mammi, S., & Peggion, E. (1990) *Biochemistry* (preceding paper in this issue)] the conformational preferences of these peptides in the presence of SDS surfactant micelles, a mimetic for biological membranes, were examined. During these studies the conformations of these peptides were investigated in aqueous solutions by circular dichroism and nuclear magnetic resonance. A large difference was observed for the two peptides. Bombolitin I lacks any observable secondary structure in aqueous solution, independent of temperature, pH, and concentration. In striking contrast, bombolitin III adopts a well-defined α-helix at concentrations greater than 1.3 mM. This is indeed surprising given the great similarity of the two peptides. The α-helix of bombolitin III is pH dependent, with a great decrease in the observed secondary structure at pH values below 3.5. This observation could only be due to the protonation of the Asp residue at the fifth position. These findings suggest that the secondary structure arises from molecular aggregation of bombolitin III through the formation of a salt bridge involving the Asp side chain. The α-helix observed at "high" concentration (>2.5 mM) has been characterized by CD and by the NOE's measured throughout a majority of the peptide. The experimentally determined structure has been energy refined with restrained molecular dynamics. The conformational results from this study are then compared with the conformations found in the presence of surfactant micelles.

Bombolitins, heptadecapeptides isolated from the venom of a bumblebee, possess a wide variety of biological functions including enhancement of the activity of phospholipase A_2 and lysis of erythrocytes and liposomes (Argiolas & Pisano, 1984). It has been postulated that these peptides with a high percentage of hydrophobic residues form amphiphilic α-helices. The amphiphilicity of course could lead to the interaction of these peptides with membranes. To examine this question, we have carried out conformational analysis of bombolitins I and III in the presence of SDS[1] surfactant micelles (Bairaktari et al., 1990). The results from circular dichroism, high-resolution nuclear magnetic resonance, and computer simulations were quite conclusive for the presence of a large percentage of helical character.

During this study, we examined the peptides in aqueous solutions and were surprised to find a large difference in the conformational characteristics of bombolitins I and III, despite the similarity of the sequences. The only differences going from bombolitin I to bombolitin III are $Thr^4 \rightarrow Met^4$, $Thr^5 \rightarrow Asp^5$, and $Met^6 \rightarrow Ile^6$. Here, we report the characterization of these conformational differences as examined by circular dichroism, nuclear magnetic resonance, and computer simulations, namely, NOE-restrained molecular dynamics.

Experimental Procedures

Circular dichroism (CD) spectra were obtained on a Jasco Model J-600A automatic recording spectropolarimeter according to the methods described previously (Bairaktari et al., 1990). All CD spectra were recorded at room temperature and are reported in terms of ellipticity units per mole of peptide residue ($[\theta]_R$).

The NMR experiments were performed on a Bruker AM 400 spectrometer and the data processed on a Bruker X-32 workstation. The samples were prepared at concentrations of 0.064, 2.56, and 5.1 mM peptide in either ^2H_2O (Aldrich) or H_2O (containing 10% ^2H_2O). Two-dimensional homonuclear ^{1}H NMR experiments were recorded at 40 °C with the TPPI method (Drobny et al., 1979; Bodenhausen et al., 1980) for generation of pure absorption mode spectra. The 2D homonuclear Hartmann–Hahn (HOHAHA) spectra were obtained following the methods of Bax and Davis (1985) with incorporation of a 1,1-ECHO observation for the H_2O samples (Bax et al., 1987; Sklenar & Bax, 1987). The NOESY spectra were acquired following standard procedures (Bodenhausen et al., 1984) with irradiation for suppression of the solvent signal for the H_2O samples. The data were collected and processed as previously described (Bairaktari et al., 1990).

The molecular dynamics and energy minimizations were carried out on a VAX 8650 with the XPLOR simulation package (Brünger, 1988) with the following modifications: (1) the force constant of the ω torsion was reduced from 300 to 20 kcal/mol and (2) the phase shift of the energy expression for the ϕ torsion was adjusted to obtain minima at 60°, 180°, and −60°. Both of these adjustments are in line with parameters commonly employed (Momany et al., 1975; Weiner et al., 1984; Hagler, 1985). The NOE-restrained molecular dynamics were

† This work was partially supported by the National Research Council (CNR) of Italy.

* To whom correspondence should be addressed.

‡ Present address: Laboratory of Analytical Biochemistry, University Hospital, Ioannina, Greece.

§ Present address: Organisch-Chemisches Institut, Technische Universität München, Garching, FRG.

[1] Abbreviations: NMR, nuclear magnetic resonance; CD, circular dichroism; SDS, sodium dodecyl sulfate; NOE, nuclear Overhauser enhancement; HOHAHA, homonuclear Hartmann–Hahn spectroscopy; NOESY, two-dimensional nuclear Overhauser enhancement spectroscopy; cmc, critical micellar concentration.

0006-2960/90/0429-10097$02.50/0

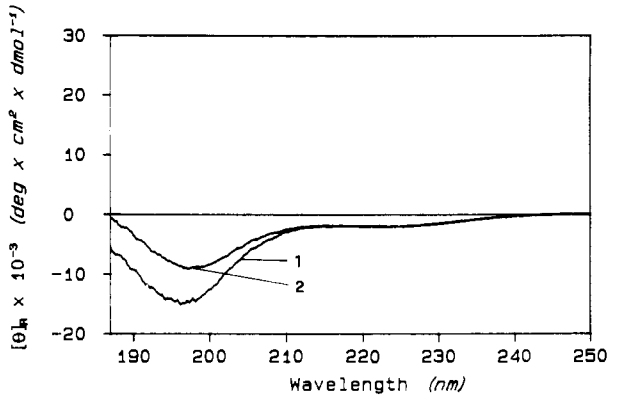

FIGURE 1: CD spectra of bombolitin I (2.72×10^{-5} M) in H_2O at pH 3.06 (1) and pH 9.04 (2).

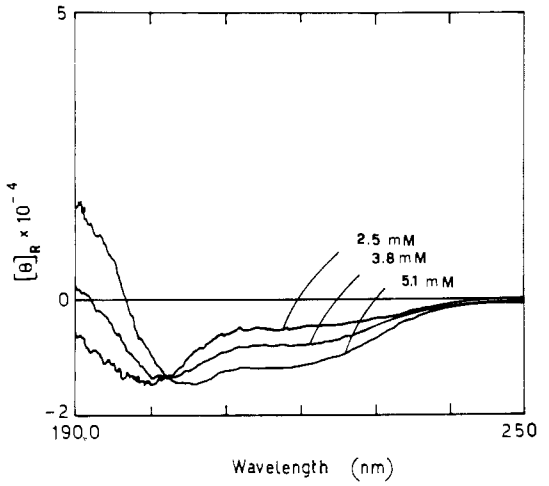

FIGURE 2: CD spectra of bombolitin I in aqueous solution at pH 7.3 at various concentrations (indicated).

carried out for 20 ps, preceded by a 2-ps equilibration period allowing for the application of the NOE's as previously described (Bairaktari et al., 1990). The simulation was continued for 10 ps without the NOE constraints to examine the energetics of the structure obtained.

Results and Discussion

The CD spectra of bombolitin I in dilute aqueous solution at acid and basic pH values are shown in Figure 1. They clearly indicate the absence of ordered secondary structure, which is practically pH independent. As the concentration is increased, only minor differences are observed up to 2.56 mM (Figure 2). At the highest concentration employed (5.12 mM), a small increase of ordered conformation is observed. The band at 222 nm is an indication of the presence of α-helix.

The CD spectra of dilute solutions of bombolitin III are also indicative of mostly disordered structure. In this case there is little pH dependence up to pH 8.5 (data not shown). At very basic conditions (pH $\geq$11) there is an increase of order, probably due to deprotonation of the charged lysine side chains.

A much greater variability is found in the CD spectra at pH 4.5 as a function of concentration than for bombolitin I (Figure 3). At a concentration of 1.28 mM, the CD spectrum already indicates the formation of α-helix. At 2.56 mM, the helix content is of the order of 60%, while bombolitin I is completely random. The increase in the amount of secondary structure with concentration illustrates the molecular aggregation of bombolitin III, probably occurring through the hydrophobic surface of the helix. At the highest concentration employed (6.4 mM) the content of α-helix is apparently reduced, due to precipitation of the aggregates (data not shown). The aggregation process of the amphiphilic peptide is similar to micelle formation in a detergent solution at concentrations above the cmc. In the case of bombolitin III at pH 4.5 the change of molar ellipticity as a function of peptide concentration is S-shaped (Figure 4) and indicates that the "critical" peptide concentration for the formation of aggregates of helices is $\geq$1 mM. While in normal detergent solutions micelle formation occurs through interaction of the hydrophobic moiety of amphiphilic *molecules*, in this case aggregate formation occurs through hydrophobic interactions of amphiphilic *structures*.

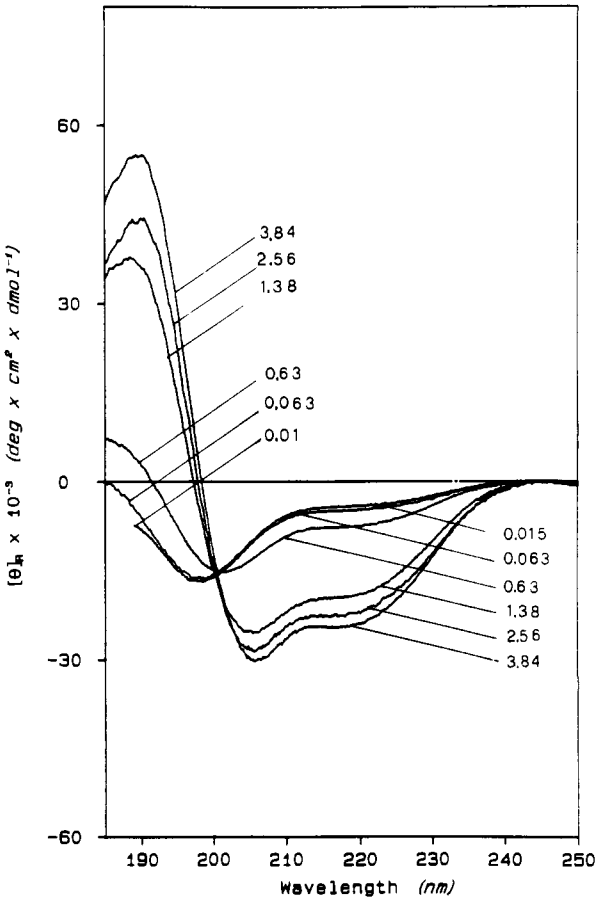

FIGURE 3: CD spectra of bombolitin III in aqueous solution at pH 4.5 at various concentrations (mM, indicated).

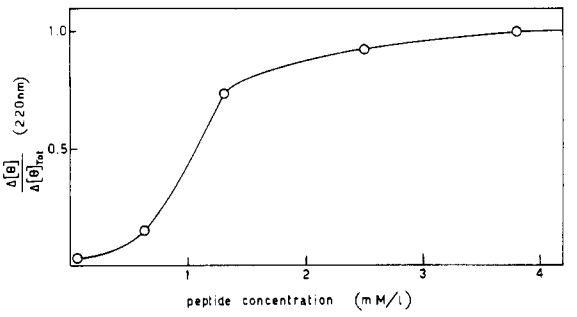

FIGURE 4: Relative change of molar ellipticity of bombolitin III at 220 nm in aqueous solution at pH 4.5 as a function of the peptide concentration.

The effect of pH on the aggregation of bombolitin III is illustrated in Figure 5. At a concentration of 2.56 mM, the conformation is strongly pH dependent. At pH values above 3.5, the helical content is for the most part maintained. Below this pH, the aggregation and subsequent formation of α-helix are greatly reduced.

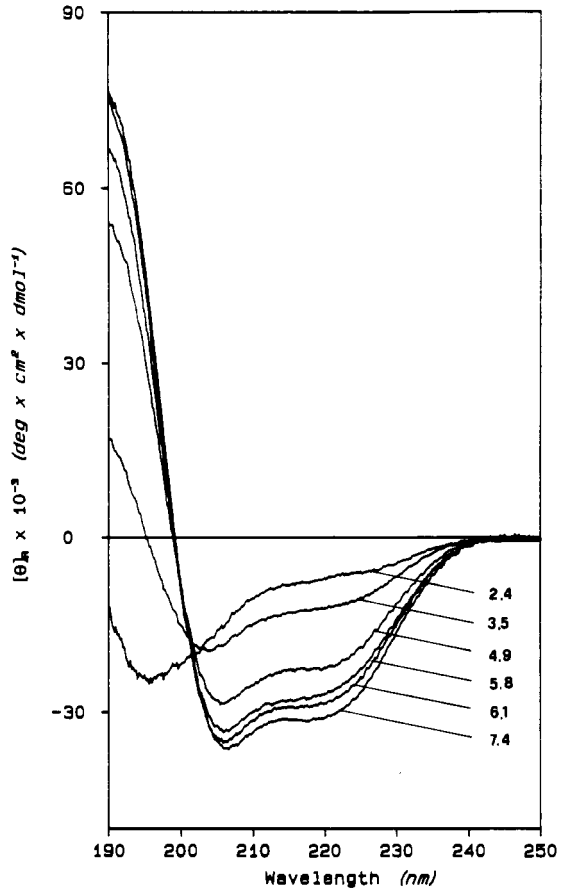

FIGURE 5: CD spectra of bombolitin III in aqueous solution (2.56 mM) at various pH values (indicated).

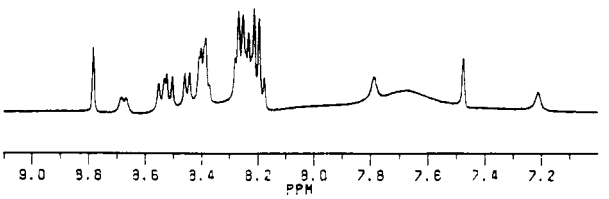

FIGURE 6: ^1H NMR spectrum of 2.56 mM bombolitin I in H_2O, pH 4.5.

From the one-dimensional proton NMR spectra of the peptides, similar conclusions can be drawn. The amide region of bombolitin I at 2.56 mM in H_2O shows sharp, well-resolved resonances (Figure 6). The NMR spectra of bombolitin III in H_2O at various concentrations are shown in Figure 7. At 0.063 mM, similar to the spectrum of bombolitin I, well-resolved resonances are observed. At a concentration of 2.56 mM, there is a severe broadening of the amide resonances. However, only a single set of lines are observed, indicative of a single conformation of the peptide (or averaging of many conformers, fast on the NMR time scale). With increasing concentration, up to 5.12 mM, multiple resonances are observed: the previous broad peaks and many additional broad and sharp resonances.

The observed differences between bombolitin I and bombolitin III with regard to self-aggregation must be due to the amino acid sequence. The two peptides differ in the amino acids at positions 4–6: -Thr-Thr-Met- for bombolitin I and -Met-Asp-Ile- for bombolitin III. Since at pH less than 3 the aggregation and consequent helix formation of bombolitin III are substantially reduced and the only change taking place is the protonation of the carboxylate function of the Asp residue at position 5, we conclude that this side chain stabilizes the

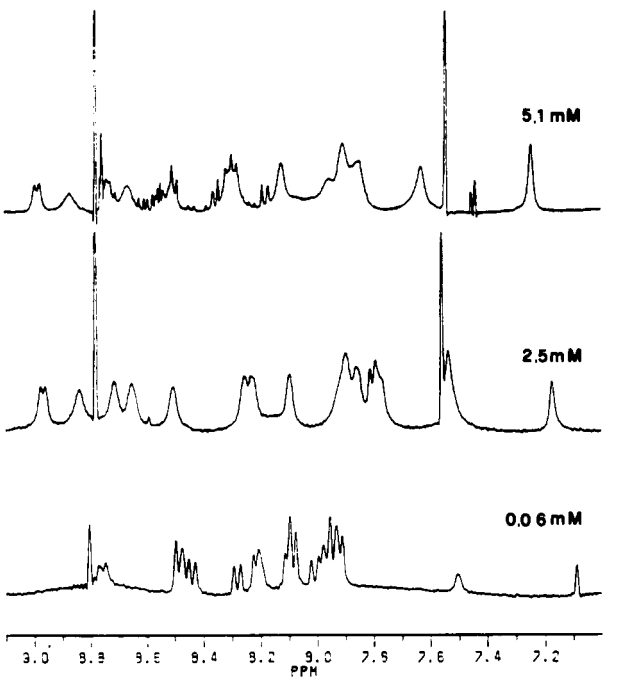

FIGURE 7: ^1H NMR spectra of bombolitin III in H_2O, pH 4.5, at various concentrations.

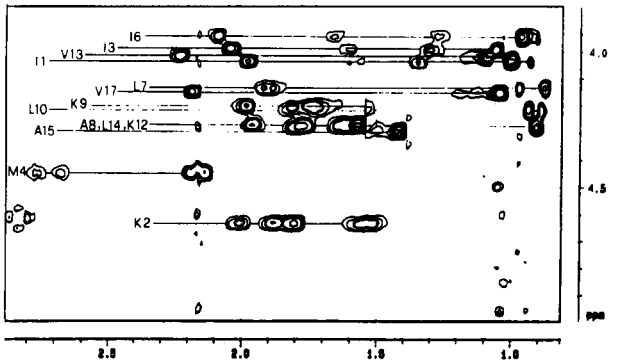

FIGURE 8: Expanded portion of the two-dimensional homonuclear Hartmann–Hahn spectrum of 2.5 mM bombolitin III in ^2H_2O illustrating the $C^{\alpha}H$ to aliphatic region.

formation of the α-helix, possibly through the formation of a salt bridge.

To better understand this phenomenon (and since bombolitin I exhibits a much-reduced tendency to aggregate in aqueous solution), we have concentrated our efforts on the conformational characterization of bombolitin III. However, it should be noted that in the presence of SDS micelles bombolitin I adopts a well-defined α-helix, not dissimilar to that found for bombolitin III under similar conditions (Bairaktari et al., 1990).

The resonance assignment of bombolitin III at 2.56 mM in water was carried out with HOHAHA and NOESY experiments. The $C^{\alpha}H$ and aliphatic region of the pure-phase absorption HOHAHA spectrum in ^2H_2O is shown in Figure 8. The mixing time is sufficient for transfer of magnetization up to ^6J, allowing for the identification of each of the spin systems present. The HOHAHA spectrum in H_2O, shown in Figure 9, was furthermore used for the assignment of the amide resonances. The differentiation of the redundant amino acids and sequential assignment was achieved with the observed NOE's of which the interresidue $C^{\alpha}H(i) \rightarrow NH(i+1)$, $NH(i) \rightarrow NH(i+1)$, and $C^{\beta}H(i) \rightarrow NH(i+1)$ are the most important. In Figures 10 and 11, spectra illustrating these assignments are shown.

Table I: Observed Nuclear Overhauser Effects for Bombolitin III in Aqueous Solution[a]

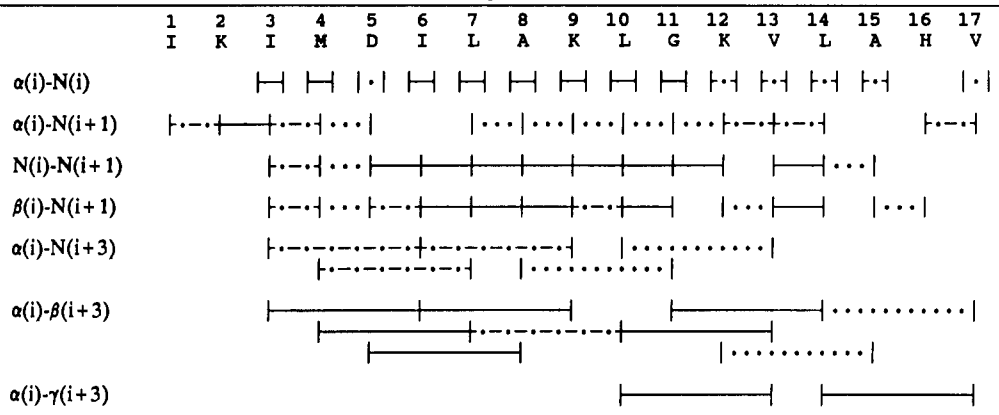

[a] Strength of NOE calculated from volume of the cross peak observed in NOESY spectra: (—) strong; (-·-) medium; (···) weak.

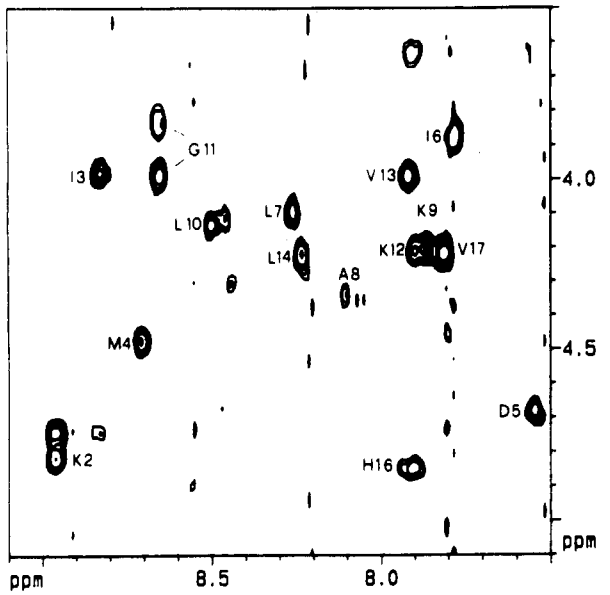

FIGURE 9: Fingerprint region of the two-dimensional homonuclear Hartmann–Hahn spectrum of 2.5 mM bombolitin III in 90% H_2O (10% ^2H_2O).

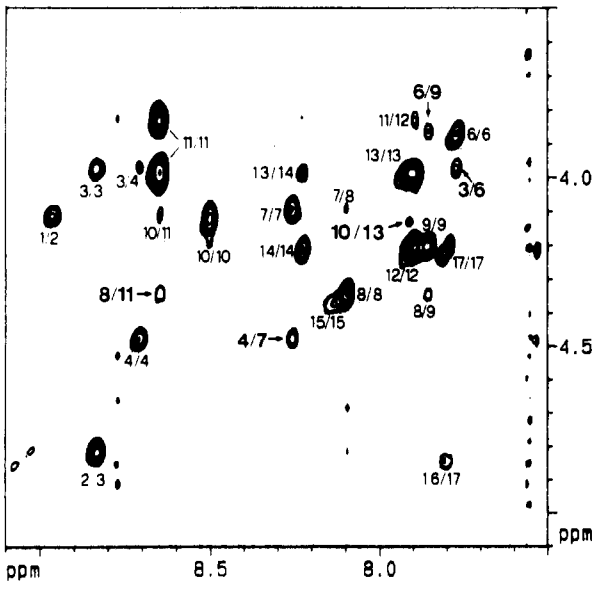

FIGURE 10: Fingerprint region of the two-dimensional pure-phase absorption NOESY spectrum of 2.5 mM bombolitin III in 90% H_2O (10% ^2H_2O). A mixing time of 200 ms was used. The NOE's between $C^{\alpha}H(i) \rightarrow NH(i)$, $C^{\alpha}H(i) \rightarrow NH(i+1)$, and $C^{\alpha}H(i) \rightarrow NH(i+3)$ are labeled.

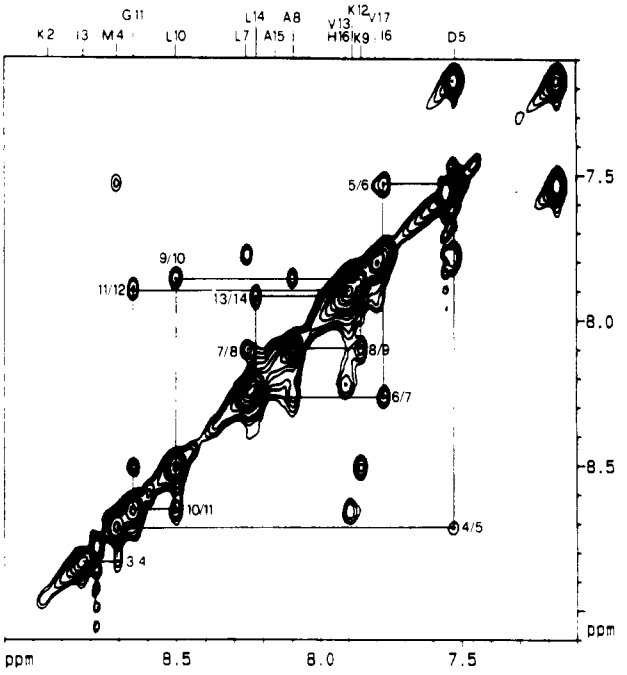

FIGURE 11: Expanded portion of the two-dimensional pure-phase absorption NOESY spectrum of 2.5 mM bombolitin III in 90% H_2O (10% ^2H_2O). A mixing time of 200 ms was used.

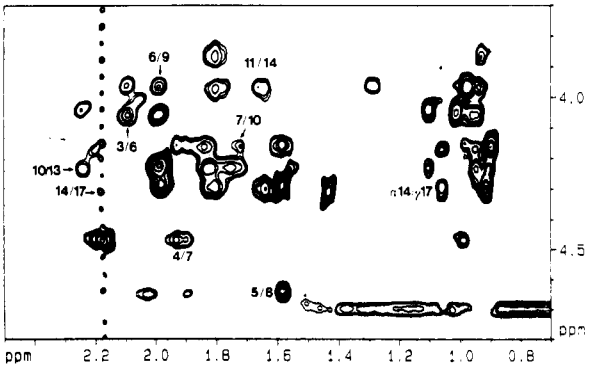

FIGURE 12: Expanded portion of the two-dimensional pure-phase absorption NOESY spectrum of 2.5 mM bombolitin III in ^2H_2O. A mixing time of 200 ms was used. The NOE's between $C^{\alpha}H(i) \rightarrow C^{\beta}H(i+3)$ extending from residue 3 to residue 17 are illustrated.

In addition to the sequential assignments, the NOESY spectra also show numerous short distances between amino acid residues in positions i and $i+3$ [$C^{\alpha}H(i) \rightarrow NH(i+3)$ and $C^{\alpha}H(i) \rightarrow C^{\beta}H(i+3)$], many of which are illustrated in Figures

10 and 12. These through-space connectivities provide strong evidence for the presence of an α-helix extending from residue 3 to residue 17 (Wüthrich et al., 1984). The NOE data are summarized in Table I.

The results from CD and NMR clearly indicate the presence of a large extent of α-helical character of bombolitin III at 2.56 mM. To refine the experimentally generated structure, NOE-restrained molecular dynamics simulations were carried out, starting from a completely α-helical structure. Since the goal of the simulations is the refinement of the structure under the experimental conditions employed and not the determination of the global minimum, the experimental data are of great utility in defining the starting structure. The restraints utilized in the simulations are listed in Table I.

The suitability of the starting structure is illustrated by the large number of NOE's satisfied. The RMS difference between the target distances and the actual distance between the atoms involved in the NOE's is 0.25 Å. The structure obtained after the equilibration period and slow application of the NOE's satisfies all of the constraints.

The structure obtained after 20 ps of molecular dynamics has an RMS difference of the NOE constraints and target values of 0.10 Å. The central portion of the α-helix is well maintained during the dynamics. In Table II, the ϕ, ψ, and χ_1 values of the structure are given. The backbone torsions of residues 3–15 are indicative of the secondary structure. The unwinding of the helix at the N-terminus is consistent with the observed NOE's; the NOE's characteristic for the α-helix begin at residue 3. The unwinding at the C-terminus indicates that the $C^{\alpha}H(14)$ to $C^{\beta}H(17)$ and the $C^{\alpha}H(14)$ to $C^{\gamma}H(17)$ NOE's are not sufficient to maintain the secondary structure during the dynamics. Only with the addition of the constraints NH(i) to NH(i+1) and $C^{\alpha}H(i)$ to NH(i+3) is the α-helix maintained during the simulation.

The extension of the simulation for 10 ps without the NOE restraints resulted in minor changes in the conformation of bombolitin III. The torsion angles after this period are given in Table II. The RMS differences between this structure and that after the first 20 ps is 1.39 Å (0.78 Å for residues 3–15). It can be concluded that the application (and fulfillment) of the NOE restraints did not cause great conformational distortions deemed energetically unfavorable.

A comparison of the conformations obtained for bombolitin III in aqueous solution at 2.56 mM and in the presence of SDS micelles shows very small differences. The RMS difference of all the atoms of the structures from the molecular dynamics is 0.77 Å (0.32 Å for residues 3–15). In both cases, the measured NOE's, characteristic for α-helices, e.g., (i) → (i+3), have been measured for a majority of the peptide. The location and intensity of the CD bands also indicate similar characteristics. Interestingly, the length of the helical segment in the aggregates is almost the same as that of a single molecule in SDS.

The α-helix of bombolitin III is amphiphilic. It is therefore not surprising to find that in aqueous solutions these helices self-associate, through hydrophobic attractions. However, there are many questions that need to be addressed, such as the number of helices (molecules of bombolitin III) that make up the aggregate and the relative orientation of the helices within the aggregate.

Attempts to characterize the manner of the molecular aggregation of bombolitin III have as yet been unsuccessful. The careful examination of NOESY spectra indicates only intramolecular NOE's; no obvious intermolecular cross peaks are observed. Even experiments with long mixing times (from 300 to 800 ms) do not show any evidence that define the intermolecular interaction. However, the observation of such NOE's would indeed be fortuitous, given the high redundancy of amino acids and the possibility of a parallel arrangement of the helices. With such an arrangement, in fact, it would be almost impossible to differentiate between interresidue and intermolecular NOE's.

Within proteins such as phospholipase A_2 (Dijkstra et al., 1981) and uteroglobin (Morize et al., 1987), amphiphilic helices are packed in an antiparallel array via hydrophobic interactions. It is possible that a similar arrangement is formed in the aggregates of bombolitin III. Recently, there has been considerable investigation of the so-called leucine zipper, segments of DNA binding proteins with a leucine spaced every seventh residue (Landschultz et al., 1988). Mutagenesis studies have suggested that the helices associate in a parallel fashion (Landschultz et al., 1989). To examine this, Kim and co-workers (O'Shea et al., 1989) have devised model systems, forming covalent linkages between the helices. From examination of these model systems the orientation of the helices

Table II: Selected Dihedral Torsions (deg) of Bombolitin III from Molecular Dynamics Simulations

		structures from molecular dynamics	
residue	torsion	after 20 ps	extended for 10 ps
Ile[1]	ψ	170	167
	χ_1	−76	−56
Lys[2]	ϕ	−47	−44
	ψ	−28	−48
	χ_1	−51	−179
Ile[3]	ϕ	−78	−66
	ψ	−53	−46
	χ_1	−69	−60
Met[4]	ϕ	−57	−53
	ψ	−36	−52
	χ_1	−52	−45
Asp[5]	ϕ	−61	−50
	ψ	−57	−61
	χ_1	−170	164
Ile[6]	ϕ	−60	−64
	ψ	−48	−42
	χ_1	−61	−74
Leu[7]	ϕ	−60	−52
	ψ	−34	−53
	χ_1	−68	−58
Ala[8]	ϕ	−77	−56
	ψ	−43	−44
	χ_1	−63	−64
Lys[9]	ϕ	−67	−62
	ψ	−50	−58
	χ_1	−99	−99
Leu[10]	ϕ	−70	−51
	ψ	−34	−59
	χ_1	−84	−65
Gly[11]	ϕ	−54	−55
	ψ	−52	−56
Lys[12]	ϕ	−56	−64
	ψ	−48	−39
	χ_1	−174	175
Val[13]	ϕ	−53	−57
	ψ	−39	−60
	χ_1	180	173
Leu[14]	ϕ	−68	−45
	ψ	−65	−60
	χ_1	−179	−175
Ala[15]	ϕ	−79	−71
	ψ	58	52
	χ_1	−55	−71
His[16]	ϕ	−178	173
	ψ	42	−176
	χ_1	−105	−96
Val[17]	ϕ	−178	167
	χ_1	95	68

was determined. Investigations of this variety on the aggregation of bombolitin III are currently being examined within our laboratories.

Registry No. L-Asp, 56-84-8; bombolitin I, 95648-97-8; bombolitin III, 95732-42-6.

REFERENCES

Argiolas, A., & Pisano, J. J. (1984) *J. Biol. Chem. 259*, 10106–10111.

Bairaktari, E., Mierke, D. F., Mammi, S., & Peggion, E. (1990) *Biochemistry* (preceding paper in this issue).

Bax, A., & Davis, D. (1985) *J. Magn. Reson. 65*, 355–360.

Bax, A., Sklenar, V., Clore, G. M., & Gronenborn, A. M. (1987) *J. Am. Chem. Soc. 109*, 6511–6513.

Bodenhausen, G., Vold, R. L., & Vold, R. R. (1980) *J. Magn. Reson. 37*, 93–106.

Bodenhausen, G., Kogler, H., & Ernst, R. R. (1984) *J. Magn. Reson. 58*, 370–388.

Brünger, A. T. (1988) *XPLOR SOFTWARE*, President & Fellows Harvard University, Cambridge, MA.

Dijkstra, B. W., Kalk, K. H., Hol, W. G. J., & Drenth, J. (1981) *J. Mol. Biol. 147*, 97–123.

Drobny, G., Pines, A., Sinton, S., Weitekamp, D., & Wemmer, D. (1979) *Symp. Faraday Soc. 13*, 49–55.

Hagler, A. T. (1985) in *The Peptides* (Hruby, V., Udenfriend, S., & Meienhofer, J., Eds.) Vol. 7, pp 241–296, Academic Press, Orlando, FL.

Landschultz, W. H., Johnson, P. F., & McKnight, S. L. (1988) *Science 240*, 1759–1764.

Landschultz, W. H., Johnson, P. F., & McKnight, S. L. (1989) *Science 243*, 1681–1690.

Momany, F. A., McGuire, R. F., Burgess, A. W., & Scheraga, H. A. (1975) *J. Phys. Chem. 79*, 2361–2381.

Morize, I., Surcouf, E., Vaney, M. C., Epelboin, Y., Bühner, M., Fridlansky, F., Milgrom, E., & Mornon, J. P. (1987) *J. Mol. Biol. 194*, 725–739.

O'Shea, E. K., Rutkowski, R., Stafford, W. F., & Kim, P. S. (1989) *Science 245*, 646–648.

Powell, M. J. D. (1979) *Math. Programming 12*, 241–254.

Sklenar, V., & Bax, A. (1987) *J. Magn. Reson. 74*, 469–479.

Weiner, S. J., Kollman, P. A., Case, D. A., Chandra Singh, U., Ghio, C., Alagona, G., Profeta, S., & Weiner, P. (1984) *J. Am. Chem. Soc. 106*, 765–784.

Wüthrich, K., Billeter, M., & Braun, W. (1984) *J. Mol. Biol. 180*, 715–740.

Phosphorylation of Iodopsin, Chicken Red-Sensitive Cone Visual Pigment†

Yoshitaka Fukada,‡ Koichi Kokame,‡ Toshiyuki Okano,‡ Yoshinori Shichida,‡ Tôru Yoshizawa,*,‡ J. Hugh McDowell,§ Paul A. Hargrave,§,⊥ and Krzysztof Palczewski§,‖

Department of Biophysics, Faculty of Science, Kyoto University, Kitashirakawa-Oiwakecho, Sakyo-ku, Kyoto 606, Japan, Department of Ophthalmology and Department of Biochemistry and Molecular Biology, University of Florida, Gainesville, Florida 32610-0284, and Robert S. Dow Neurological Sciences, Good Samaritan Hospital & Medical Center, Portland, Oregon 97209.

Received May 22, 1990; Revised Manuscript Received July 30, 1990

ABSTRACT: The amino acid sequence has been determined for the carboxyl-terminal 41 amino acids of chicken red-sensitive cone pigment, iodopsin. This sequence is distinct from but structurally homologous to that of other visual pigments. It contains a region rich in the hydroxy amino acids serine and threonine. In the related rod cell visual pigment, rhodopsin, such serines and threonines have previously been identified as sites for phosphorylation by rhodopsin kinase. Phosphorylation of photolyzed rhodopsin serves to terminate its ability to function in visual transduction as an activator of G-protein. We have purified and reconstituted both chicken rhodopsin and chicken iodopsin and shown them to be phosphorylated by bovine rhodopsin kinase. Chicken iodopsin has a K_m and V_{max} similar to but distinguishably different from that for bovine rhodopsin. These results, in conjunction with other data, suggest that visual pigments in cone cells, upon absorption of light, undergo functional processes similar to those of the visual pigments in rod cells.

Vertebrate rod cells mediate dim-light vision in black and white, whereas cone cells are responsible for color vision. Both rods and cones contain photoreceptor visual pigments that receive light energy and initiate the photoresponses. Rod cells have been more amenable to study than cones. Rod cell visual pigment, rhodopsin, and its interacting proteins have been prepared and characterized in some detail (Falk & Applebury, 1987). Although cone cells have many similarities to rod cells, they have distinct structural differences, operate at much higher light intensities, and have a different time constant of response (Pugh & Cobbs, 1986). In order to understand the functional differences between rod and cone photoreceptor cells, it will be necessary to prepare and study the properties of proteins in the cone cell visual transduction pathway.

The rod photoreceptor proteins are members of the family of receptor proteins that function via G-proteins (Applebury & Hargrave, 1986; Dohlman et al., 1987). After rhodopsin receives light it undergoes a change in conformation that

† This work was supported in part by a Grant-in-Aid for Specially Promoted Research from the Japanese Ministry of Education, Science and Culture (to T.Y.), by a Special Coordination Fund of the Science and Technology Agency of the Japanese Government (to T.Y.), by Grants EY06225 and EY06226 and Core Facility Grants EY08571 (to P.A.H.) and EY08062 (to K.P.) from the National Eye Institute, and by an unrestricted departmental grant from Research to Prevent Blindness, Inc. (to P.A.H.). P.A.H. is Francis N. Bullard Professor of Ophthalmology.

* To whom correspondence should be addressed.

‡ Kyoto University.

§ Department of Ophthalmology, University of Florida.

⊥ Department of Biochemistry and Molecular Biology, University of Florida.

‖ Good Samaritan Hospital & Medical Center.

0006-2960/90/0429-10102$02.50/0